JVST A
Journal of Vacuum Science & Technology A

Characteristics of remote plasma atomic layer-deposited HfO_2 films on O_2 and N_2 plasma-pretreated Si substrates

Cite as: J. Vac. Sci. Technol. A **24**, 678 (2006); https://doi.org/10.1116/1.2194029
Submitted: 19 September 2005 • Accepted: 13 March 2006 • Published Online: 04 May 2006

Jihoon Choi, Seokhoon Kim, Jinwoo Kim, et al.

View Online Export Citation

ARTICLES YOU MAY BE INTERESTED IN

Effects of N_2 remote plasma nitridation on the structural and electrical characteristics of the HfO_2 gate dielectrics grown using remote plasma atomic layer deposition methods
Journal of Vacuum Science & Technology A **24**, 900 (2006); https://doi.org/10.1116/1.2198865

Characteristics of HfO_2 thin films grown by plasma atomic layer deposition
Applied Physics Letters **87**, 053108 (2005); https://doi.org/10.1063/1.2005370

Plasma enhanced atomic layer deposition of HfO_2 and ZrO_2 high-k thin films
Journal of Vacuum Science & Technology A **23**, 488 (2005); https://doi.org/10.1116/1.1894666

J. Vac. Sci. Technol. A **24**, 678 (2006); https://doi.org/10.1116/1.2194029 **24**, 678

Characteristics of remote plasma atomic layer-deposited HfO_2 films on O_2 and N_2 plasma-pretreated Si substrates

Jihoon Choi, Seokhoon Kim, Jinwoo Kim, Hyunseok Kang, and Hyeongtag Jeon[a]
Division of Materials Science and Engineering, Hanyang University, Seoul 133-791, Korea

Choelhwyi Bae
System LSI division, Samsung Electronics Co., Ltd., Yongin Gyeonggi-do 449-711, Korea

(Received 19 September 2005; accepted 13 March 2006; published 4 May 2006)

Characteristics of remote plasma atomic layer-deposited HfO_2 on Si, which has a very thin SiO_2 interlayer with and without remote plasma nitridation, have been investigated. The thin ($\sim$1.5 nm) intermediate layer containing nitrogen, which was prepared by sequential O_2 and N_2 remote plasma treatment of the Si substrate, can effectively suppress growth of the unintentional interface layer. In addition, it enhances the thermal stability and the resistance to oxygen diffusion during rapid thermal annealing. The HfO_2 film containing the remote plasma nitrided SiO_2 interlayer annealed at 800 °C showed a lower equivalent oxide thickness of $\sim$1.89 nm and a lower leakage current density (3.78×10^{-7} A cm^{-2} at $|V_G - V_{FB}| = 2$ V) compared to a non-nitrided sample of the same physical thickness. Also, we compared the characteristics of HfO_2 films annealed in two different ambient environments, N_2 and O_2.
[DOI: 10.1116/1.2194029]

I. INTRODUCTION

When high-*k* materials are used as a new gate oxide instead of SiO_2, the film thickness can be increased to reduce the tunneling leakage current while scaling the equivalent oxide thickness (EOT).[1,2] Among these materials, HfO_2 films have recently received considerable attention for desirable properties such as high dielectric permittivity with low leakage current, low heat of formation (271 kcal/mol), and compatibility with Si substrates.[3] However, the postdeposition annealing process of HfO_2 films often includes growth of a parasitic or unintentional thin SiO_x interlayer or amorphous Hf-silicates through reactions at metal oxide/Si interfaces.

Nitridation of the Si substrate has been used as a promising solution for suppressing the increase of the interfacial layer to sustain low EOT values and the penetration of other impurities. Nitrogen incorporation technology has been extensively investigated in SiO_2 gate dielectrics to reduce hot-electron-induced degradation, to suppress impurity diffusion, to prevent interfacial reactions, and to improve reliability.[4] In particular, recent works on nitrided ZrO_2 indicate that the incorporation of nitrogen at the $\sim$3–5 at. % level led to improved electrical properties and thermal stability of the film, though the maximum annealing temperature was only 800 °C.[5] Recently, nitridation using a plasma can incorporate nitrogen into the dielectric film at a lower temperature (below 500 °C) than a thermal nitridation process.[6] Among these nitridation methods, remote plasma nitridation (RPN) can be applied to the HfO_2 thin film deposited by remote plasma assisted atomic layer deposition (RPALD). When the HfO_2 thin film deposited using RPALD is used in gate stacks,[7] RPN not only enhances thermal stability, but also assists in reducing the EOT together with a thin ($\sim$1 nm) Al_2O_3 interlayer.[8]

In this article, we report the effect of the RPN process on the thermal stability and electrical properties of $HfO_2/SiO_xN_y/Si$ gate stacks deposited by RPALD. $HfO_2/SiO_xN_y/Si$ gate stacks were prepared by an *in situ* three step process: (i) remote plasma oxidation (RPO) of the Si substrate to form a thin SiO_2 layer, (ii) RPN of the prepared thin ($\sim$1.5 nm) SiO_2 layer, and (iii) RPALD of the HfO_2 film.

II. EXPERIMENTAL PROCEDURES

HF-last Si (100) *p*-type substrates with a resistivity of 6–9 cm were loaded into a RPALD chamber, where *in situ* (i) RPO, (ii) RPN, and (iii) RPALD can be subsequently performed. Oxygen plasma for RPO was generated for 5 min at a power of 100 W. Nitrogen plasma for RPN was also generated for 20 min at a power of 300 W. A HfO_2 thin film was grown onto this nitrided thin SiO_2 by RPALD using a $Hf[N(C_2H_5)_2]_4$ precursor. During the RPO, the RPN, and the HfO_2 deposition, the processing pressure and temperature were maintained at 1 torr and 300 °C. Radio frequency remote plasma sources were used to minimize plasma-induced damage. The growth rate was 1.1 Å/cycle for the HfO_2 deposition by using RPALD. After the deposition process, rapid thermal annealing (RTA) was performed in N_2 or O_2 for 30 s at 600–1000 °C, respectively. Angle-resolved x-ray photoelectron spectroscopy (ARXPS) was performed on deposited samples by an Al $K\alpha$ x-ray source (1.486 keV) at angles of 30°, 60°, and 90° with respect to the sample surface. Auger electron spectroscopy (AES) was also performed. To fabricate metal oxide semiconductor (MOS) capacitors, Pt electrodes were deposited on the HfO_2 films

---

[a] Author to whom correspondence should be addressed; electronic mail: hjeon@hanyang.ac.kr

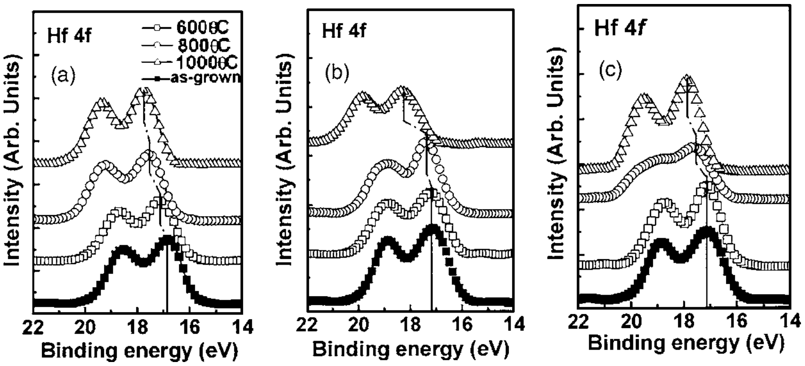

FIG. 1. XPS spectra of Hf 4*f* core levels for the as-grown HfO_2 sample (a) without and [(b) and (c)] with RPN were observed, obtained after rapid thermal annealing treatment at a temperature of 600–1000 °C for 30 s. (a) HfO_2(3.5 nm)/SiO_2(1.5 nm) annealed in N_2 ambient, (b) HfO_2(3.5 nm)/SiO_xN_y(1.5 nm) annealed in N_2 ambient, and (c) HfO_2(3.5 nm)/SiO_xN_y(1.5 nm) annealed in O_2 ambient.

through a shadow mask using an *e*-beam evaporation system. After forming gas (3% H_2/ 97% N_2) and annealing at 450 °C for 30 min, capacitance-voltage (*C*-*V*) measurements were performed using a Keithley 590 *C*-*V* analyzer at 100 kHz. Current-voltage (*I*-*V*) measurements were also performed using an HP4155A semiconductor parameter analyzer. High-resolution transmission electron microscopy (HRTEM) was used to study the interface structure in the dielectric stacks.

III. RESULTS AND DISCUSSION

A. Effect of RPN on thermal stability

Figure 1 shows normalized Hf 4*f* core level spectra of HfO_2 samples: (i) as-grown, (ii) annealed at 600 °C, (iii) 800 °C, and (iv) 1000 °C for 30 s. First consider the N_2-annealed samples shown in Figs. 1(a) and 1(b). The Hf 4*f* peak of the HfO_2 sample without RPN [Fig. 1(a)] gradually shifts to a higher binding energy. Compared with these shifts, the HfO_2 sample with RPN [Fig. 1(b)] shows a negligible shift of the Hf 4*f* spectra after RTA at 600 and 800 °C. This peak shift of the sample without RPN indicates the formation of Hf-silicate with Si–O–Hf bonding states, because the binding energy of the Hf 4*f* peak for Hf-silicate shifts to a higher binding energy than that for HfO_2.[9] Therefore, we think that nitrogen incorporation into the intentionally formed thin SiO_2 layer plays an important role in suppressing the formation of Hf-silicates during the postdeposition anneal. We can suppose that the formation of the Si–N bonding states occurs in the Si–SiO_2 interfacial region,[10] and that this Si–N bonding may suppress the formation of Hf-silicate. Previous research reports that the formation of Hf-silicate[11,12] is due to Si diffusion into the growing HfO_2 film and oxygen diffusion into the Si substrate resulting in the formation of SiO_2 (Ref. 13) in contrast with the thermodynamic data reported by Hubbard and Schlom.[14] Figure 1(c), which gives the spectrum for when RTA was performed in O_2 ambient, will be discussed in Sec. III B.

Figure 2 shows cross-sectional HRTEM images of HfO_2 samples (a) with RPN and (b) without RPN annealed at 600 °C for 30 s in O_2 ambient. The incorporating small amounts of N atoms in a thin oxide was successfully accomplished by the RPN process. The incorporated N concentration in the oxide was approximately 5 at. % and it investigated by AES (not shown here). It was confirmed that the presence of nitrogen significantly improved the thermal stability of the films with respect to crystallization.

The structure of the HfO_2 film without RPN changed from amorphous to polycrystalline after RTA at 600 °C, while the HfO_2 film with RPN retained its amorphous structure. It is believed that a reaction between the HfO_2 film and nitrogen incorporated into the SiO_2 interfacial layer may occur even at relatively low temperatures. For the HfO_2 sample with RPN, a relatively thin (~1.5 nm) interfacial layer is observed, compared with the sample without RPN (~1.8 nm). These results indicate that the RPN treatment effectively enhances the immunity to oxygen diffusion during RTA resulting in the growth of the interfacial layer. Furthermore, the difference between O_2 ambient and N_2 ambient for the HfO_2 samples with RPN is negligible during RTA at 600 °C.

Figure 3 shows the change of EOT and leakage current density of HfO_2 MOS samples with increasing temperature. For the as-grown samples, the obtained EOT and leakage current density are (i) 1.80 nm and 6.7×10^{-8} A/cm^{-2} for the "with RPN" and (ii) 2.09 nm and 4.1×10^{-7} A/cm^{-2} for "without RPN." Additionally, the EOT and leakage current density of with RPN samples were always lower than those of without RPN samples after RTA at 600–1000 °C. In the HfO_2 sample with RPN, the small increase in EOT with increasing annealing temperature is due to the nitrogen incorporation by RPN, which suppresses the growth of the interlayer. It is noteworthy that the leakage current density of with RPN samples is reduced by about one order of magnitude as compared to without RPN samples, despite the reduced EOT of the with RPN samples.

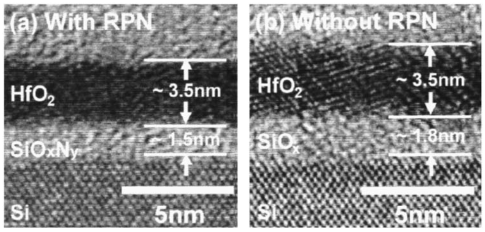

FIG. 2. Cross-sectional HRTEM images of HfO_2 sample with and without RPN after annealing at 600 °C for 30 s in O_2 ambient: (a) HfO_2 (~3.5 nm)/SiO_xN_y(~1.5 nm)/Si and (b) HfO_2(~3.5 nm)/SiO_x (~1.8 nm)/Si.

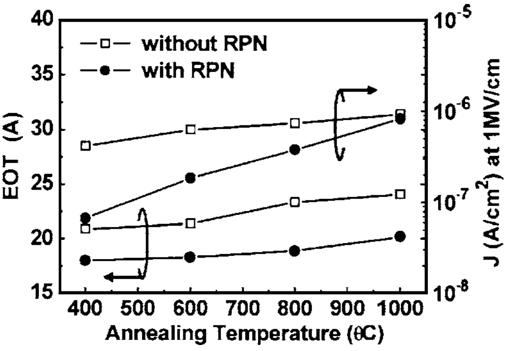

FIG. 3. Variation of the EOT and leakage current density for the HfO_2 sample with and without RPN as a function of annealing temperature after RTA for 30 s in N_2 ambient.

B. Effect of postdeposition anneal in O_2 ambient

In this section, we compare the characteristics of HfO_2 samples with RPN annealed in two different ambient environments, N_2 and O_2. As shown in Fig. 1(c), the Hf 4*f* peak for the HfO_2 sample with RPN annealed in the O_2 ambient shifted to a higher binding energy after RTA at 800 °C than the sample annealed in the N_2 ambient [Fig. 1(b)]. This shift of the Hf 4*f* peak indicates the growth of an interfacial layer during RTA in the O_2 ambient. To investigate these results more intensively, ARXPS was performed on two with RPN samples annealed at 800 °C in N_2 and O_2 ambient, respectively. The samples were measured at take-off angles of 30°, 60°, and 90°. At 90° with respect to the surface plane, the signal from the interfacial layer is maximized relative to that from the HfO_2 layer. At small angles, the signal from the interfacial layer becomes greatly enhanced, relative to that from the HfO_2 layer. Therefore, HfO_2 layer and the interfacial layer are enhanced at take-off angles of 30° and 90°, respectively.

As shown in Fig. 4(a), the ARXPS oxygen 1*s* spectra of a with RPN sample were clearly deconvoluted into two binding energy components after RTA at 800 °C in N_2 ambient. The main peak of the oxygen 1*s* spectra with two chemical states at 530.0 eV is attributed to the oxygen 1*s* spectra from HfO_2. The shoulder at ~531.5–531.8 eV is attributed to Hf-silicate (Hf–O–Si) bonds introduced during RTA. The electronegativity of the silicon atom (1.90) in the Hf-silicate layer is relatively higher than that of the Hf atom (1.30), so a replacement of the Si second-nearest neighbor shifts the binding energy higher. The HfO_2 sample without RPN showed a more significant increase of Hf-silicate (Hf–O–Si) bonds compared with the HfO_2 sample with RPN. The increase of the Hf-silicate bonds with a take off angle can be derived from the growth of the interfacial layer during RTA. It was also observed from the HRTEM that the growth of the interlayer in the HfO_2 sample with RPN is much less than the same sample without RPN (Fig. 2).

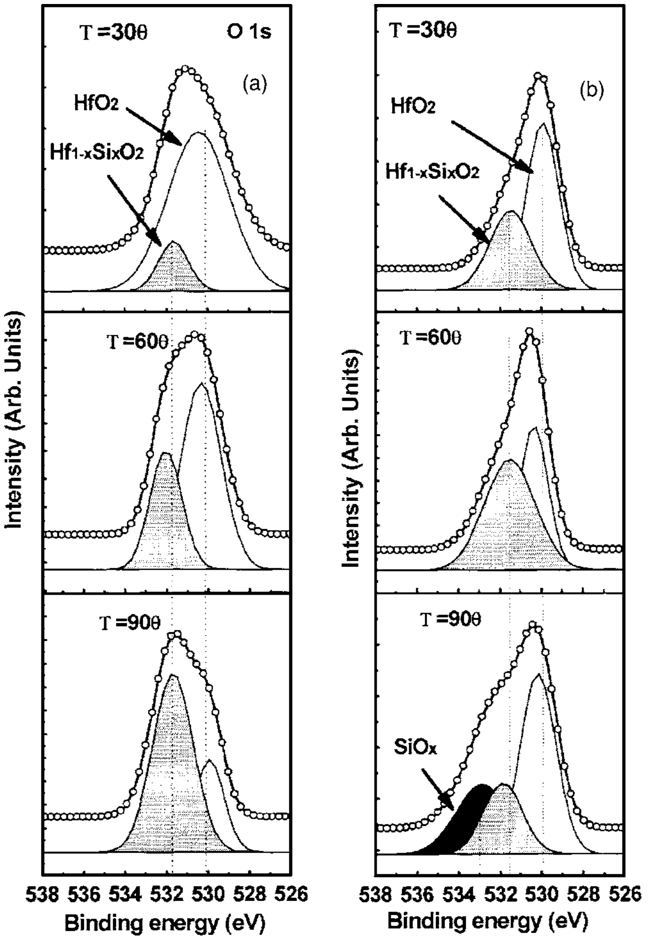

FIG. 4. Angle-resolved XPS spectra of oxygen 1*s* core levels for the 5 nm HfO_2 sample with RPN, obtained after rapid thermal annealing treatment at a temperature of 800 °C for 30 s in (a) N_2 or (b) O_2 ambient. The samples were measured at take off angles of 30°, 60°, and 90°.

Similar chemical shift features were also observed for the oxygen 1*s* spectra of the with RPN sample annealed in O_2 ambient, as shown in Fig. 4(b). The ARXPS oxygen 1*s* spectra of the HfO_2 sample with RPN were clearly deconvoluted into three binding energy components, namely, HfO_2, Hf-silicate at a 1.5 eV shift, and SiO_x at a 2.7 eV shift. The oxygen 1*s* spectra at a take off angle of 90° showed a component (dark area) at a 2.7 eV shift from the main peak. This shift suggests that the component is attributed to the SiO_x layer formed in the interfacial region after RTA in O_2 ambient.

The EOT of the sample annealed in O_2 ambient abruptly increased after RTA at 800 °C, as shown in Table I. The correlation between the ARXPS and the EOT indicates that RTA at 800 °C in O_2 ambient leads to the growth of the SiO_x layer and significantly decreases the effect of RPN. In addition, the V_{FB} shifted negatively for the sample with RPN annealed in O_2 ambient. This shift resulted from the enhanced hole trapping associated with the modified SiO_x interlayer.

IV. CONCLUSIONS

In conclusion, we investigated the thermal stability and electrical characteristics of $HfO_2/SiO_xN_y/Si$ gate stacks using ARXPS, HRTEM, *C-V*, and *I-V* analyses. Compared with the HfO_2 sample without RPN, the sample with RPN

TABLE I. EOT, leakage current, flatband voltage, and effective charges for the three different samples used in this study

RPN	Anneal	Anneal temperature (°C)	EOT (nm)	Leakage (10^7 A/cm^2)	V_{FB} (V)
Without	N_2	As grown	2.0	4.1	0.3
		600	2.1	6.3	0.4
		800	2.3	7.4	0.4
With	N_2	As grown	1.8	0.6	0.5
		600	1.8	1.8	0.5
		800	1.9	3.7	0.6
With	O_2	As grown	1.8	0.7	0.5
		600	1.8	1.9	0.4
		800	2.0	7.6	0.3

suppressed the growth of an undesired interfacial layer during annealing. The nitrogen incorporated into the interfacial layer can also stabilize the gate stacks in an amorphous structure during RTA. $HfO_2/SiO_xN_y/Si$ gate stacks showed lower EOT and leakage current density, compared with a $HfO_2/SiO_2/Si$ gate dielectric. Therefore, these results suggest that the RPN pretreatment enhances the thermal stability and the electrical characteristics of HfO_2 thin films deposited by RPALD.

ACKNOWLEDGMENTS

This work was supported by the National Program for Tera-level Nanodevices of the Ministry of Science and Technology as one of the 21st century Frontier Programs.

[1] G. D. Wilk, R. M. Wallace, and J. M. Anthony, J. Appl. Phys. **89**, 5243 (2001).
[2] S. Thompson, P. Packan, and M. Bohr, Intel Technology Journal Q3'98.
[3] S. Gopalan, K. Onishi, R. Nieh, C. S. Kang, R. Choi, H.-J. Cho, and J. C. Lee, Appl. Phys. Lett. **80**, 4416 (2000).
[4] H. S. Momose, T. Morimoto, Y. Ozawa, K. Yamabe, and H. Iwai, IEEE Trans. Electron Devices **41**, 546 (1995).
[5] S. Jeon, C.-J. Choi, T.-Y. Seong, and H. Hwang, Appl. Phys. Lett. **79**, 245 (2001).
[6] P. Chen, H. B. Bhandari, and T. M. Klein, Appl. Phys. Lett. **85**, 1574 (2004).
[7] J. Kim, S. Kim, C. Bae, and H. Jeon, Appl. Phys. Lett. **87**, 053108 (2005).
[8] M. Park, J. Koo, J. Kim, C. Bae, and H. Jeon, Appl. Phys. Lett. **86**, 252110 (2005).
[9] M.-H. Cho, Y. S. Roh, C. N. Whang, and K. Fujihara, Appl. Phys. Lett. **81**, 472 (2002).
[10] T. Nishimura, T. Okazawa, Y. Hoshino, and A. Toriumi, Appl. Phys. Lett. **96**, 6113 (2004).
[11] B. K. Park, J. Park, M. Cho, C. S. Hwang, K. Oh, Y. Han, and D. Y. Yang, Appl. Phys. Lett. **80**, 2368 (2002).
[12] P. D. Kirsch, C. S. Kang, J. Lozano, J. C. Lee, and J. G. Ekerdt, J. Appl. Phys. **91**, 4353 (2002).
[13] D. G. Schlom and J. H. Haeni, MRS Bull. **27**, 198 (2002).
[14] K. J. Hubbard and D. G. Schlom, J. Mater. Res. **11**, 2757 (1996).